Received: 3 December 2023 | Revised: 20 February 2024 | Accepted: 27 February 2024

DOI: 10.1111/jce.16244

ORIGINAL ARTICLE

WILEY

Endocardial repolarization dispersion in BrS: A novel automatic algorithm for mapping activation recovery interval

Sara Latrofa MD[1] | Valentina Hartwig Eng D[2] | Lorenzo Bachi Eng D[1] | Pasquale Notarstefano MD[3] | Silvia Garibaldi MD[4] | Luca Panchetti MD, PhD[4] | Martina Nesti MD[4] | Paolo Seghetti Eng D[1,2] | Umberto Startari MD, PhD[4] | Gianluca Mirizzi MD, PhD[4] | Maria Sole Morelli Eng D, PhD[4] | Martina Modena MSc, PhD[1] | Andrea Mazzanti MD, PhD[5] | Michele Emdin MD, PhD[1,4] | Alberto Giannoni MD, PhD[1,4] | Andrea Rossi MD[4]

[1]Health Science Interdisciplinary Center, Scuola Superiore Sant'Anna, Pisa, Italy

[2]Institute of Clinical Physiology, Pisa, Italy

[3]Cardiovascular and Neurological Department, San Donato Hospital, Arezzo, Italy

[4]Fondazione Toscana Gabriele Monasterio, Pisa, Italy

[5]Department of Molecular Medicine, University of Pavia, Pavia, Italy

Correspondence
Sara Latrofa, Scuola Superiore Sant'Anna, Piazza Martiri della Libertà 33, Pisa, Italy.
Email: s.latrofa@santannapisa.it

Disclosures: None.

Abstract

Introduction: Repolarization dispersion in the right ventricular outflow tract (RVOT) contributes to the type-1 electrocardiographic (ECG) phenotype of Brugada syndrome (BrS), while data on the significance and feasibility of mapping repolarization dispersion in BrS patients are scarce. Moreover, the role of endocardial repolarization dispersion in BrS is poorly investigated. We aimed to assess endocardial repolarization patterns through an automated calculation of activation recovery interval (ARI) estimated on unipolar electrograms (UEGs) in spontaneous type-1 BrS patients and controls; we also investigated the relation between ARI and right ventricle activation time (RVAT), and T-wave peak-to-end interval (Tpe) in BrS patients.

Methods: Patients underwent endocardial high-density electroanatomical mapping (HDEAM); BrS showing an overt type-1 ECG were defined as OType1, while those without (latent type-1 ECG and LType1) received ajmaline infusion. BrS patients only underwent programmed ventricular stimulation (PVS). Data were elaborated to obtain ARI corrected with the Bazett formula (ARIc), while RVAT was derived from activation maps.

Results: 39 BrS subjects (24 OType1 and 15 LTtype1) and 4 controls were enrolled. OType1 and post-ajmaline LType1 showed longer mean ARIc than controls (306 ± 27.3 ms and 333.3 ± 16.3 ms vs. 281.7 ± 10.3 ms, $p = .05$ and $p < .001$, respectively). Ajmaline induced a significant prolongation of ARIc compared to pre-ajmaline LTtype1 (333.3 ± 16.3 vs. 303.4 ± 20.7 ms, $p < .001$) and OType1

Abbreviations: ARI, activation recovery interval; ARIc, activation recovery interval corrected for the Bazett formula; ARIQ3, activation recovery interval at the 75% of the distribution corrected for the Bazett formula; BrS, Brugada syndrome; EAM, electroanatomical mapping; ECG, electrocardiogram; EPS, electrophysiological study; HDEAM, high-density right ventricular electroanatomical mapping; ICD, implantable cardioverter-defibrillator; LAT, local activation time; LType1, latent type-1 electrocardiographic pattern during electrophysiological study; OType1, overt type-1 electrocardiographic pattern during electrophysiological study; PVS, Programmed ventricular stimulation; **PVS+**, ventricular tachycardia/fibrillation inducible during programmed ventricular stimulation; PVS-, ventricular tachycardia/fibrillation not inducible during programmed ventricular stimulation; ROI, region of interest; RV, right ventricle; RVAT, right ventricular activation time; RVOT, right ventricular outflow tract; SCD, sudden cardiac death; Tpe, Tpeak-Tend interval; Tpec, Tpeak-Tend interval corrected for the Bazett formula; UEG, unipolar electrogram; VF, ventricular fibrillation; VGD, voltage gradient dispersion; VT, ventricular tachycardia.

(306 ± 27.3 ms, $p < .001$). In patients with type-1 ECG (OTtype1 and post-ajmaline LType1) ARIc correlated with RVAT ($r = .34$, $p = .04$) and Tpec ($r = .60$, $p < .001$), especially in OType1 subjects ($r = .55$, $p = .008$ and $r = .65$ $p < .001$, respectively).

Conclusion: ARIc mapping demonstrates increased endocardial repolarization dispersion in RVOT in BrS. Endocardial ARIc positively correlates with RVAT and Tpec, especially in OType1.

KEYWORDS

activation recovery interval, Brugada syndrome, electroanatomic substrate, endocardial mapping, repolarization dispersion, Tpeak-Tend interval

1 | INTRODUCTION

Brugada syndrome (BrS) is defined by the presence of a coved-type J-point elevation in right precordial leads on surface electrocardiogram (ECG) and is characterized by an increased risk of sudden cardiac death (SCD).[1] Both depolarization and repolarization abnormalities have been described in BrS patients, and their interplay with regard to the electrophysiological basis of the disease is controversial.[2] Previous clinical studies suggested that a varying degree of J-point elevation observed in different BrS patients may reflect right ventricular outflow tract (RVOT) different conduction abnormalities, as well as repolarization heterogeneity.[3]

The repolarization hypothesis states that both the ECG phenotype and arrhythmogenic mechanism may be due to transmural and epicardial repolarization dispersion in BrS.[2] Tpeak-Tend (Tpe) interval is widely used as an index of transmural dispersion of repolarization.[4] A recent meta-analysis has shown that Tpe prolongation is associated with higher arrhythmic risk in BrS patients, although a cut-off value to identify high-risk patients still needs to be defined.[5] Activation recovery interval (ARI) estimates action potential duration[6] and has previously been used to evaluate spatial repolarization dispersion in BrS.[7–11] However, data on the significance and feasibility of repolarization dispersion mapping in BrS patients are scarce. Moreover, the role of endocardial repolarization dispersion on BrS electrical substrate is poorly investigated.

Therefore, we aimed to: (1) evaluate endocardial repolarization dispersion using an automated calculation of ARI from endocardial unipolar electrograms (UEGs) derived from RV high-density electroanatomic mapping (RV-HDEAM) in BrS patients and controls; (2) investigate the relation between ARI distribution and RV activation, as well as Tpeak-Tend interval (Tpe) in BrS patients with type-1 phenotype.

2 | MATERIALS AND METHODS

2.1 | Study population

The methods of the study are summarized in Figure 1. Consecutive BrS patients with previously documented spontaneous type-1 patterns were enrolled. Matched healthy patients undergoing EPS for atrioventricular nodal reentrant tachycardia, atrioventricular reciprocating tachycardia, or atrial fibrillation/flutter provided control data. Exclusion criteria were: the presence of overt cardiac structural disease, age <16 years, and informed consent denial. The diagnosis of BrS was based on current recommendations.[12,13] Genetic testing was performed using Illumina Nextera TruSight™ Cardio Sequencing kit on an Illumina NextSeq™ 550 system (Illumina). All patients underwent an electrophysiological study (EPS) combined with RV endocardial HDEAM using the CARTO®3 system (Biosense Webster Inc.). Patients showing an overt type-1 ECG during EPS were defined OType1; those without were defined LType1 and received ajmaline challenge[13] during HDEAM. All BrS subjects underwent PVS after RV-HDEAM (in the LType1 subgroup, PVS was performed after complete recovery of ECG modifications induced by ajmaline). The induction protocol was carried out from RV apex and RVOT at two drive trains (eight stimuli at 600 and 400 ms) with up to two extrastimuli until refractoriness or a 200-ms coupling interval was reached.[14] PVS was considered positive (PVS+) when the patient developed VF, VT lasting >30 s or requiring direct current shock because of hemodynamic instability. Noninducible patients were defined as PVS−.

All participants provided written informed consent for the study. The study was conducted following the 2013 Helsinki Declaration.

2.2 | HDEAM data export and ARI calculation

RV-HDEAM was performed during sinus rhythm using the CARTO®3 (Biosense Webster Inc.) mapping system, as previously described.[15] A linear multipolar DecaNav® catheter with 2-8-2 interelectrode spacing was used for RV mapping. The 11th electrode of DecaNav® catheter was used as unipolar reference. An ablator catheter with a force sensor (SmartTouch®, Biosense Webster Inc.) was then used to verify the validity of electrograms obtained with the mapping catheter. Confidense®mapping software (Biosense Webster Inc.) was set to acquire exclusively points having position stability ≤6 mm, LAT stability ≤6 ms, pattern matching with sinus rhythm

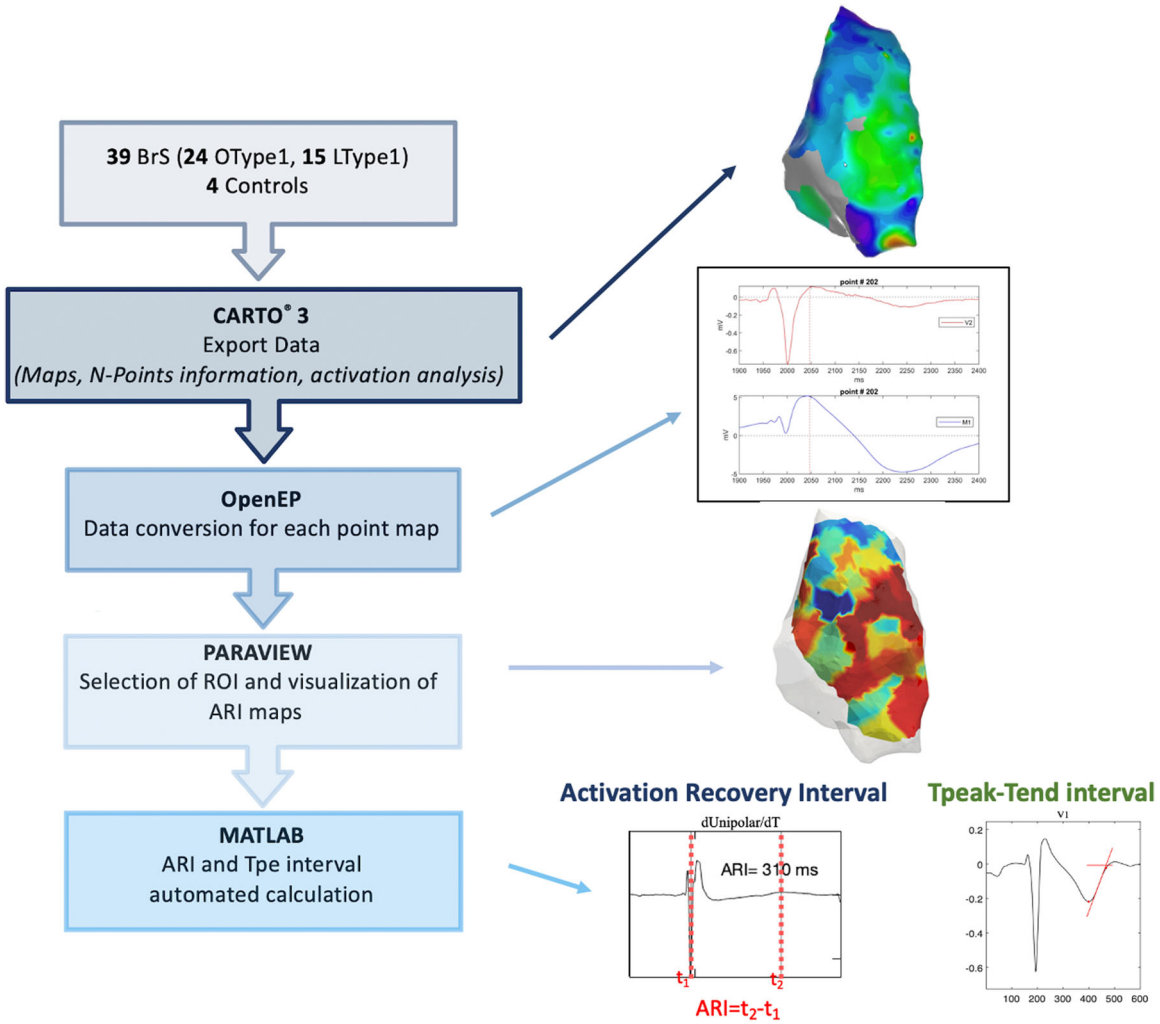

FIGURE 1 Workflow for data export and calculation. Workflow summarizing the process used to export data from the CARTO®3 system, to analyze it, and to calculate ARI and Tpe for each BrS patient and each control subject. See the main text for more details. ARI indicates activation recovery interval; BrS, Brugada syndrome; LType1, latent type-1 Brugada patient; OType1, overt type-1 Brugada patient; ROI, region of interest; Tpe, Tpeak-Tend interval.

pattern and contact force 5–25 g. The Fill&Color® interpolation threshold for electroanatomical mapping was set at 6 mm. A minimum of 700 points were acquired.

Unipolar signals were filtered at 1–240 Hz. Amplitude, duration, relation to surface QRS, and multiple components of the signals were simultaneously analyzed. For each patient, local activation maps (LATs) were used to calculate right ventricular activation time (RVAT), defined as the interval between the beginning of surface QRS and the latest depolarizing point in RV.

Data acquired during RV-HDEAM were exported and OpenEP software[16] was used to convert data into MatLab® (MathWorks Inc.) format. Paraview software provided the selection of a specific region of interest (ROI) in RVOT. MatLab® was used to create an automated algorithm for ARI calculation using endocardial UEGs at each point of the ROI. ARI was calculated starting from the minimum dV/dt of the unipolar QRS to the maximum dV/dt of the following T wave, as previously described by Wyatt.[6] In case of noise, the presence of a premature ventricular beat, or abnormal T-wave morphologies, the UEG was discarded.

For each patient, the mean ARI corrected for heart rate according to the Bazett formula (ARIc) was calculated. ARIQ3 refers to the ARIc value at 75% of ARIc distribution; the ARIQ3 extension (as the percentage with respect to the whole ROI) was also calculated. These two parameters were used to address and compare between groups the regions having the longest repolarization; furthermore, the ARIQ3 extension highlights the topographic representation of the zones having the highest depolarization dispersion into the ROI. ARI values of each point were interpolated using Paraview[17] on a three-dimensional mesh. A color code was set for a specific ARI duration to create ARIc maps. A two-color map was created by setting the threshold at ARIQ3 to visualize the spatial extension of ARIQ3 for each patient.

2.3 | Tpeak-Tend interval calculation

Tpeak-Tend interval (Tpe) was calculated only in BrS with type-1 ECG phenotype (OType1 and post-ajmaline LType1). Tpe was measured on 20 low-noise beats recorded during the procedure using a multi-stage, dedicated automated algorithm.

For Tpe calculation, data was exported from the CARTO®3 system to MatLab®. Using MatLab®, heartbeat detection on surface ECG was first performed, and heart rate was determined. Non-sinus beats were discarded through morphological clustering. Twenty low-noise sinus beats were then extracted and averaged, obtaining an average beat for each lead. Tpe was calculated on V1, V2, and V3 (which mainly reflect RV repolarization),[18] using an algorithm based on the tangent method.[5] An operator checked the accuracy of the calculation of each Tpe value with a custom graphic user interface, correcting the starting/ending point of the interval if needed or discarding the lead if Tpe was not measurable due to abnormal T wave morphology. For each patient, the mean value of Tpe of V1, V2, and V3 was calculated. Mean corrected Tpe (Tpec) was determined using the Bazett formula.

2.4 | Treatment and follow-up

ICD implantation for primary prevention was proposed to PVS+ and to selected PVS− patients with familial history and suspicious symptoms. Patients underwent follow-up with ECG monitoring and half-yearly ICD check in recipients unless symptoms appearance, arrhythmias documentation, or ICD intervention.

2.5 | Statistical analysis

Continuous variables were reported as mean ± standard deviation or median and interquartile range according to the data distribution, assessed with the Shapiro test. Discrete variables were expressed as numbers and/or percentages.

For comparison between two groups, unpaired *t* test or nonparametric Mann–Whitney *U* test was used depending on the variable distribution. ANOVA or Kruskal–Wallis, with Tukey's range test, was used to compare more than two groups. For the comparison of a group before and after ajmaline injection, paired *t* test or Wilcoxon test was used as appropriate. Correlation between continuous variables was tested using Pearson R correlation coefficient or Spearman coefficient, as appropriate, and corrected using the Benjamini–Hochberg (BH) procedure.

Differences were considered significant when p value ≤ .05. Statistical analysis and graphs were performed using R software (version R 2023.03.1+446, R Development Core Team).

TABLE 1 Clinical features of the study population.

	BrS (n = 39)	OType1 (n = 24)	LType1 (n = 15)
Age	41 ± 11	41 ± 11	41 ± 12
Male (%)	33 (85)	21 (88)	12 (80)
Family history of BrS (%)	6 (15)	3 (13)	2 (13)
Family history of SCD (%)	7 (18)	4 (17)	3 (20)
VT/VF during follow-up (%)	2 (5)	1 (4)	1 (7)
Syncope (%)	12 (31)	6 (25)	6 (40)
ICD (%)	19 (49)	13 (54)	6 (40)
Appropriate shock (%)	1 (3)	–	1 (7)
Inappropriate shock (%)	1 (3)	1 (4)	–
Infection (%)	1 (3)	1 (4)	–

Note: Data presented as mean ± standard deviation.

Abbreviations: BrS, Brugada Syndrome; ICD, implantable cardioverter-defibrillator; LType1, latent type-1 phenotype; OType1, overt type-1 phenotype; SCD, sudden cardiac death; VF, ventricular fibrillation; VT, ventricular tachycardia.

3 | RESULTS

3.1 | Study population

The study population included 39 BrS patients and 4 controls (Table 1). The selection process of BrS patients is summarized in Supporting Information: Figure A.1 and that of controls in Supporting Information: Figure A.2. BrS population included 24 OType1 patients (62%) and 15 LType1 (38%). Nine patients (23%) had VT/VF inducible at PVS (7,29%, OType1; 2,13%, LType1, p = .06). Genetic testing was performed on 30 patients, 2 (7%) carrying a *SCN5A* pathogenic mutation.

3.2 | Endocardial mapping analysis, ARI, and Tpe calculation

On average, 959 points per map were acquired during HDEAM. ARI analyses are summarized in Table 2 and Figure 2. Among BrS patients studied during type-1 ECG pattern, both post-ajmaline LType1 and OType1 showed longer ARIc values compared to controls (333.3 ± 16.3; and 306 ± 27.3 vs. controls: 281.7 ± 10.3 ms, p = .02 and p = .05, respectively). Ajmaline induced a significant prolongation of ARIc as compared either to pre-ajmaline LType1 (303.4 ± 20.7 vs. 333.3 ± 16.3 ms, p < .001) or OType1 (306 ± 27.3 vs. 333.3 ± 16.3 ms, p = .001) subjects. Ajmaline administration determined a prolongation

TABLE 2 Electrophysiological data of the study population.

	Controls ($n = 4$)	OType1 ($n = 24$)	Pre-ajmaline LType1 ($n = 15$)	Post-ajmaline LType1 ($n = 15$)
Mean ARIc, ms	281.7 ± 10.3	306 ± 27.3	303.4 ± 20.7	333.3 ± 16.3
Mean ARIQ3, ms	312.7 ± 15.1	335.1 ± 28.3	331.7 ± 23.3	366.2 ± 20.2
ARIQ3 area, % ROI	22.8	23.1	22.1	21.9
RVAT, ms	75 (7.5)	111 (44.3)	89 (13)	101 (22.5)
Tpec, ms	–	78.3 ± 12.8	–	98.4 ± 12.9

Note: Data presented as mean ± standard deviation, or median (interquartile range).

Abbreviations: ARIc, activation recovery interval corrected for the Bazett formula; ARIQ3, activation recovery interval at the 75% of the distribution corrected for the Bazett formula; LType1, latent type-1 Brugada patient; OType1, overt type-1 Brugada patient; ROI, region of interest; RVAT, right ventricular activation time; Tpec, Tpeak-Tend interval corrected for the Bazett formula.

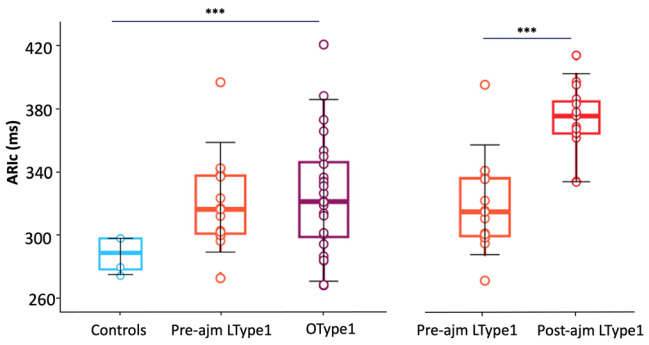

FIGURE 2 Boxplot of ARIc differences between groups. Boxplot showing the differences of ARIc between controls, pre-ajmaline LType1 and OType1 (left panel), and pre-ajmaline and post-ajmaline LType1 patients (right panel). OType1 patients had significantly longer ARIc values compared to controls ($p = .05$). No significant differences were observed between pre-ajmaline LType1 and controls, nor between OType1 and LType1. Ajmaline administration determined a significant prolongation of ARIc in LType1 patients ($p < .001$). Ajm, ajmaline; ARIc, activation recovery interval corrected for the Bazett formula; LType1, latent type-1 Brugada patient; OType1, overt type-1 Brugada patient.

of individual mean ARIc in all but one patient. Through the interpolation of ARIc values, ARIc maps were reconstructed (Figure 3).

ARIQ3 analysis is reported in Table 2. ARIQ3 analysis revealed localized longer ARIc mainly in the anterior and subpulmonary portion of RVOT (Figure 4). In controls, ARIQ3 zones had shorter ARIc values than BrS subjects (312.7 ± 15.1 vs. 347.1 ± 29.5 ms, $p = .03$). In OType1 subjects, ARIQ3 was 335.1 ± 28.3 ms and the ARIQ3 area was 23.1% of the whole ROI. In LType1 patients, ajmaline induced significant prolongation of ARIQ3 (331.7 ± 23.3 vs. 366.2 ± 20.2 ms, $p = .002$), but the extension of ARIQ3 values did not differ between pre- and post-ajmaline administration (22.1% vs. 21.9%, $p = .85$).

PVS− patients had an ARIc of 318.5 ± 24.3 ms and an ARIQ3 of 349.2 ± 26.4 ms; PVS+ patients had an ARIc of 309.8 ± 35.5 ms and an ARIQ3 of 339.8 ± 39.1 ms. There were no differences for ARIc nor ARIQ3 between these two groups ($p = .48$ and $p = .61$, respectively).

RVAT values are summarized in Table 2. No significant differences in RVAT between OType1 and pre-ajmaline LType1 ($p = .19$) were found. Considering LType1 subjects, ajmaline administration induced a significant prolongation of RVAT (89 ± 13 vs. 101 ± 22.5 ms, $p = .02$).

Tpec values, assessed in patients with type-1 ECG pattern (OType1 and post-ajmaline LType1), are summarized in Table 2. In OType1 patients, the average Tpe was 74 ± 9.5 ms, while the average Tpec was 78.3 ± 12.8 ms. Post-ajmaline LType1 patients had an average Tpe of 86.5 ± 11.7 ms and Tpec of 98.3 ± 12.9 ms. A significant difference between groups was present both for Tpe and Tpec ($p = .002$ and $p < .001$, respectively).

3.3 | Correlation analysis

Correlation plots are reported in Figures 5 and 6. In OType1 patients, a linear correlation was found between ARIc and RVAT ($r = .55$; $p = .008$) (Figure 5), and between ARIc and Tpec ($r = .65$ with $p < .001$) (Figure 6). Considering the whole type-1 ECG BrS population, ARIc and Tpec still had a good correlation ($r = .60$; $p < .001$), while the correlation between ARIc and RVAT was significant but weak ($r = .34$; $p = .04$).

ARIc showed a stronger correlation both with RVAT and Tpec compared to ARIQ3 values, except for Tpec in OType1 patients ($r = .73$; $p < .001$).

4 | DISCUSSION

Our novel algorithm was able to evaluate in an automatic, standardized manner repolarization maps through high-density point-by-point ARI analysis on endocardial UEGs in a BrS population. The main findings are the following:

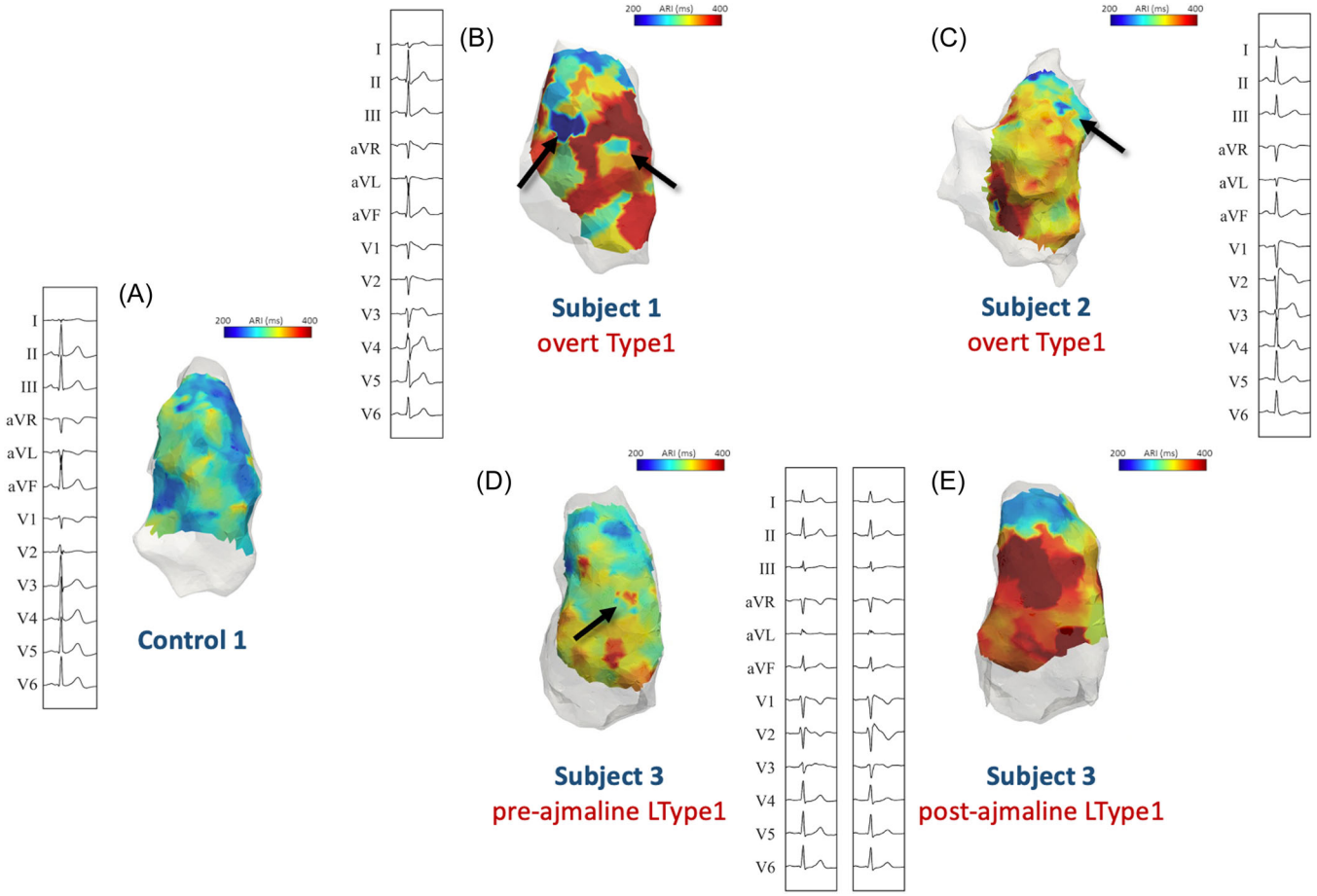

FIGURE 3 ARIc maps ARIc maps of (A) control 1 (control, mean ARIc 275.2 ms), (B) subject 1 (OType1 with an appropriate shock during follow-up, mean ARIc 323.9 ms), (C) subject 2 (OType1, mean ARIc 320.4 ms) and subject 3 (D) pre-ajmaline Ltype1 and (E) post-ajmaline LType1 (mean ARIc 301 ms and 340.7 ms). The control patient presents shorter and more homogeneous ARIc values. Ajmaline administration determines a prolongation of ARIc in subject 3. Zones of dispersion of repolarization are present in subject 1, subject 2, and subject 3 (pointed by the black arrows). ARIc, activation recovery interval corrected for the Bazett formula; BrS, Brugada Syndrome; LType1, latent type-1 Brugada patient; OType1, overt type-1 Brugada patient.

1. BrS subjects, both with latent and overt type-1 phenotype, exhibited endocardial RVOT areas presenting with marked repolarization dispersion, as highlighted by longer ARIc values compared to controls.
2. Type-1 phenotype evoked by sodium channel blockade was associated with a marked increase of endocardial repolarization dispersion coherently with a remarkable mean ARIc prolongation.
3. BrS type-1 phenotype showed prolonged ARIc values mainly in the anterior wall of RVOT.
4. A linear correlation was present between ARIc and RVAT, as well as between ARIc and Tpec in BrS patients with type-1 ECG, namely in patients with overt type-1 phenotype.

4.1 | Activation recovery interval

The repolarization hypothesis has been demonstrated in experimental models,[19] while in vivo data in BrS patients are scarce. ARI evaluated by UEGs estimates local action potential duration[6,20] and represents a measure of myocardial repolarization properties. Previous studies have demonstrated the existence of repolarization dispersion in BrS patients with type-1 ECG phenotype.[9,10] By creating high-density ARI maps, we found differences in spatial repolarization in RVOT endocardium among healthy control subjects, BrS patients with an overt type-1 pattern and those with a latent type-1 pattern. It is known that in the healthy heart, the normal propagation of the impulse generates a right ventricular apico-basal gradient of ARIs, with the early activating regions having the longest ARI and the late activating regions having the shortest. This enables a spatial synchronization of repolarization which prevents reentry phenomena.[21] ARI maps in controls (Figure 3) revealed a relatively homogenous distribution, with zones of longer ARI in the anterior part of RVOT. Both OType1 and post-ajmaline LType1 subjects exhibited significantly longer mean ARIc and localized ARIQ3 values than control subjects. Ajmaline administration induced a significant prolongation of ARIc and a marked increase of localized ARIc, as

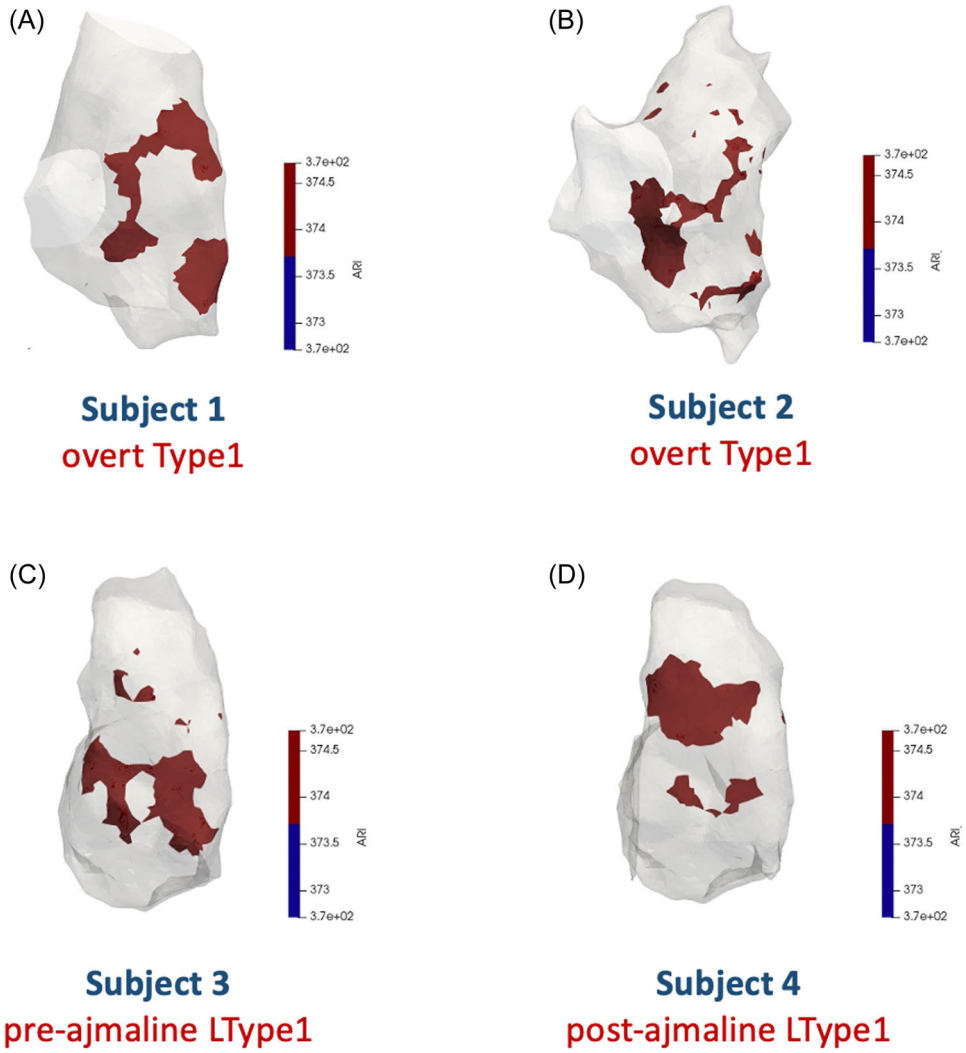

FIGURE 4 ARIQ3 maps. ARIQ3 maps of subject 1 (A) (OType1 with an appropriate shock during follow-up), (B) subject 2 (OType1), and subject 3 (pre-ajmaline LType1 (C) and post-ajmaline LType1 (D). ARIQ3 zones are specifically located in the anterior and subpulmonary portions of RVOT. ARIQ3, activation recovery interval at 75% of the ARI distribution corrected for the Bazett formula; BrS, Brugada Syndrome; LType1, latent type-1 Brugada patient; OType1, overt type-1 Brugada patient.

represented by ARIQ3 analysis. Our findings are in line with other studies demonstrating an impact of RVOT repolarization dispersion on the genesis of type-1 phenotype in BrS.[9,20] Nagase et al.[9] assessed ARIc from UEGs in the endocardial and epicardial RVOT of 19 BrS subjects undergoing pilsicainide; they reported an ARIc prolongation after pilsicainide administration specifically in epicardial RVOT, but not in the endocardium. We found, instead, a significant impact of ajmaline administration in endocardial ARI dispersion. This could be explained by the increase in spatial resolution provided by a high density of points analyzed (on average, 959 per map), which allowed a detailed repolarization map. Furthermore, a possible aggregation of action potentials in the epi-endocardial layers may create a sort of "averaging effect"; moreover, since the myocardium acts as a syncytium, changes in the endocardium might be influenced by epicardial action potential modification.

Considering type-1 phenotype populations, we observed that patients undergoing ajmaline infusion presented significantly longer ARIc values than those with spontaneous BrS patterns. It is known that a prolongation of ARIc may be due to the presence of an increase in transient potassium outward current, which produces a deep phase-1 notch and a preferential epicardial prolongation of action potentials (depending on the extent of the phase-0 depolarization upstroke). Such current is mainly expressed in RVOT rather than other RV or left ventricle zones in BrS subjects.[9] The significant ARIs prolongation after sodium-channel blockade compared to OType1 could be due to the extent of the sodium channels inactivated, which determines a consequent different impact on the transient potassium outward current: while in spontaneous type-1 subjects, only a part of these channels might be inactive, in ajmaline-induced type-1 pattern all sodium channels available could be blocked provoking a sort of "extremization response."

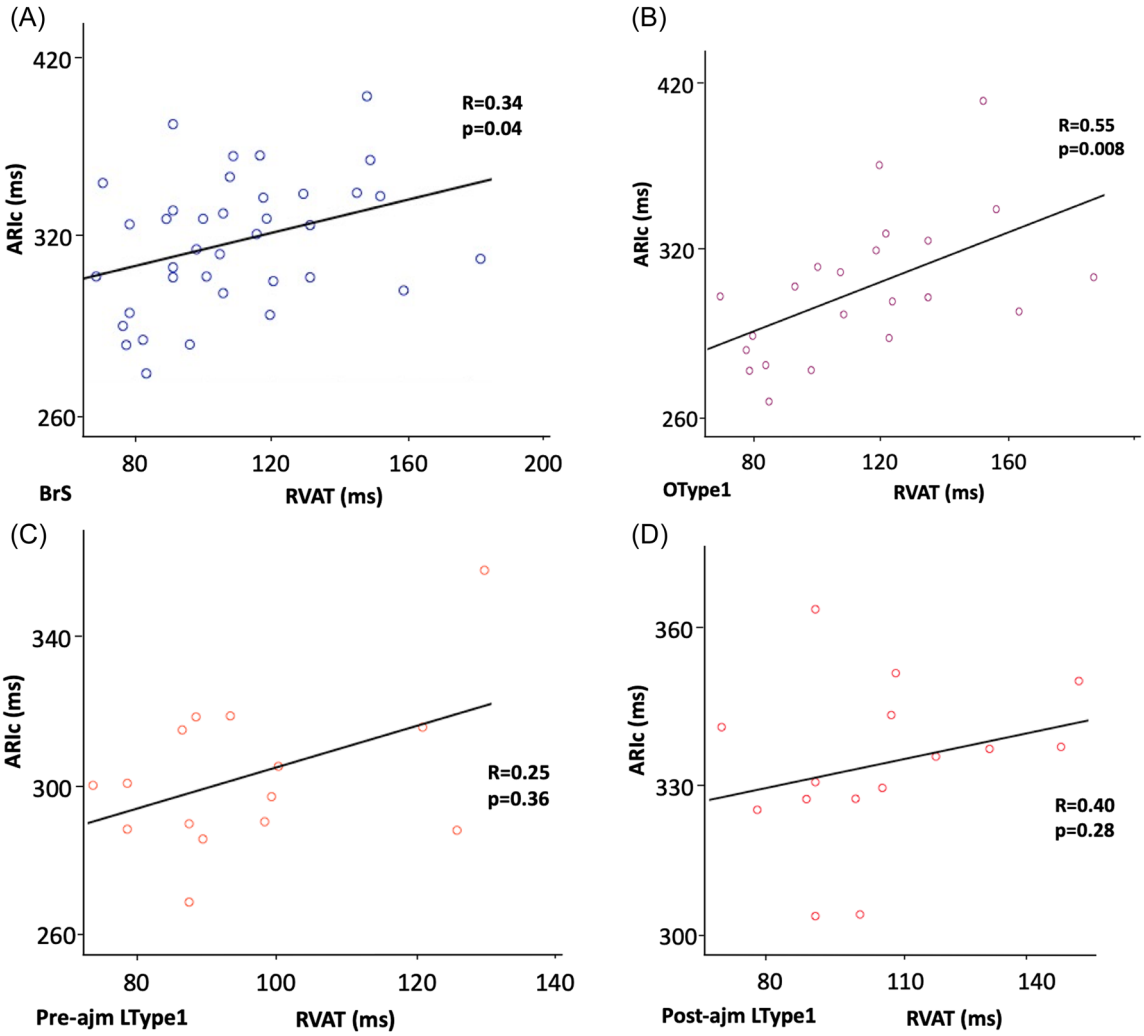

FIGURE 5 Correlation plots between RVAT and ARIc. Correlation graphs between RVAT and ARIc in (A) patients during type-1 BrS pattern (OType1 + post-ajmaline LType patients), (B) OType1 patients, (C) pre-ajmaline LType patients and (D) post-ajmaline LType patients. A significant correlation between these variables was seen in the whole type-1 BrS population ($r = .34$ $p = .04$) and especially in OType1 patients ($r = .55$ $p < .008$). Ajm, ajmaline; ARIc, activation recovery interval corrected for the Bazett formula; BrS, Brugada Syndrome; LType1, latent type-1 Brugada patient; OType1, overt type-1 Brugada patient; RVAT, right ventricular activation time.

4.2 | Correlation analysis

Considering BrS population with type-1 ECG (OType1 and post-ajmaline LType1 subjects), a linear correlation was found between ARIc and RVAT ($r = .34$; $p = .038$). The significance of this correlation increased considering patients with spontaneous type-1 phenotype ($r = .54$; $p = .008$). No correlation between ARIc and RVAT was found in post-ajmaline LType1 subjects. The relationship between RV conduction abnormalities and repolarization dispersion in BrS has been poorly investigated in the literature. Some studies supported the conclusion that BrS phenotype was generated by conduction delay in RVOT, as depolarization dispersion assessed through localized ARI prolongation in RVOT was not related to J-point elevation on ECG.[11] The authors concluded that the presence of localized conduction slowing, late, and fragmented potentials in the epicardial RVOT was secondary to conduction delays, supporting the "depolarization hypothesis."[21,22] Other authors observed a predominant role of repolarization abnormalities: the association of localized "loss of dome" during phase-1 and prolongation of action potential in other zones may induce a concealed phase-2 reentry, which accounted for epicardial fractionated and late potentials.[23,24] Our data confirm the relationship between repolarization dispersion and RV conduction in OTtype1 patients, but do not enable us to determine whether the former is caused by the latter—or vice versa. No correlation was observed between ARIc and RVAT in post-ajmaline LType1.

This study shows a significant linear correlation between ARIc and Tpec ($r = .60$; $p < .001$) in the whole type-1 ECG BrS population. This correlation is mainly driven by OType1 patients ($r = .65$ with $p < .001$) while no relationship between ARIc and Tpe was seen in post-ajmaline LType-1 subjects. Yan and Antzelevitch were the first to suggest the use of the Tpe interval as a measure of transmural dispersion of repolarization.[19] Given that Tpe interval is an accepted marker of repolarization dispersion, the good linear correlation

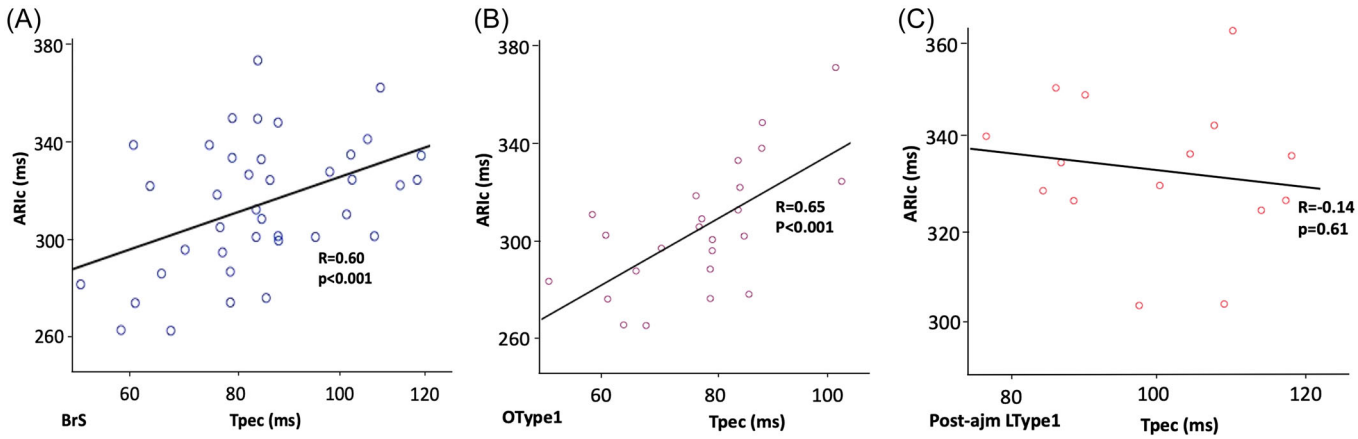

FIGURE 6 Correlation plots between Tpec and ARIc. Graphs showing the correlation between Tpec and ARIc in (A) patients during type-1 BrS pattern (OType1 + post-ajmaline LType patients), (B) OType1 patients, and (C) post-ajmaline LType patients. A significant correlation between the variables was seen in the whole type-1 BrS population ($r = .60$ $p < .001$) and especially in OType1 patients ($r = .65$ $p < .008$). Ajm, ajmaline; ARIc, activation recovery interval corrected for the Bazett formula; BrS, Brugada Syndrome; LType1, latent type-1 Brugada patient; OType1, overt type-1 Brugada patient; Tpec, Tpeak-Tend interval corrected for the Bazett formula.

between Tpec and ARIc observed in our study confirms the reliability of our model in the high-density repolarization mapping. This concept is furthermore supported by the good correlation between ARIQ3 and Tpec ($r = .73$; $p < .001$).

Clinical studies have demonstrated that Tpe prolongation was significantly associated with a high risk of ventricular tachyarrhythmias and/or SCD in BrS.[25] Moreover, a recent meta-analysis including 1740 BrS patients demonstrated that high-risk BrS individuals present longer Tpe intervals.[5] Interestingly, the presence of a linear correlation between ARIc and Tpec especially in OType1 patients seems coherent with the known prognostic role of spontaneous type-1 ECG pattern.

Finally, no significant differences in ARIc were seen when considering PVS+ and PVS− patients. Both patients of our cohort who experienced arrhythmic events during follow-up were PVS−; one patient received appropriate ICD intervention while the other refused the ICD implant and died suddenly due to VF. This observation is in line with previous studies that questioned the role of PVS alone in the prognostic evaluation of BrS patients[26] paving the way to a multiparametric model of risk stratification considering clinical and electrophysiological parameters, especially in asymptomatic BrS with a spontaneous type-1 ECG.

Since BrS is an epicardial disease, further studies are needed to address the role of endocardial repolarization dispersion, and in particular, whether it is a component of the BrS electrical substrate directly involved in arrhythmogenicity or it could be used to indirectly assess the electrical epicardial disease.

4.3 | Study limitations

Epicardial mapping was not performed and ARIs were estimated from endocardial unipolar electrograms; as BrS abnormalities are mainly detected in RVOT epicardium and have been linked to arrhythmogenesis in the syndrome, the absence of a direct epicardial ARI assessment might limit the clinical implication of the present study. Automatic ARIc and Tpec calculation still require the inspection of an operator to check possible pitfalls due to signal artifacts or T wave flattening. Background noise was responsible for discarding one lead in eight cases for Tpe calculation. The low rate of *SCN5A* mutation carriers did not allow a selective evaluation of ARIs in this group. Furthermore, regarding the study population, a broader control group could improve the study's generalizability and a higher number of arrhythmic events at follow-up could elucidate the prognostic role of endocardial ARIc prolongation.

5 | CONCLUSION

ARIc mapping through a high-density endocardial UEG automated analysis demonstrates an increase in local repolarization dispersion in RVOT of BrS subjects. In BrS patients with type-1 ECG, especially in OType1, ARIc positively correlates with abnormal RV depolarization and repolarization dispersion on surface ECG (through Tpe analysis), unveiling the location and the extension of abnormal electrical substrate. Further studies are needed to evaluate the prognostic impact of ARI mapping in a multiparametric model including other clinical and electrophysiological parameters, especially in asymptomatic BrS patients.

ACKNOWLEDGMENTS

The authors would like to thank Nicola Vanello, Andrea Ripoli, Alessandro Tognetti, Niccolò Biasi, and Davide Tirabasso for the engineering support. The authors are also grateful to Giacomo Mansi, Giuseppe Vergaro, Andrea Barison, Claudio Passino, Maurizio Pieroni, and Marcello Piacenti for their expertise and assistance throughout all the clinical aspects of the project.

DATA AVAILABILITY STATEMENT

The data that support the findings of this study are available from the corresponding author upon reasonable request.

ETHICS STATEMENT

The study was conducted following the 2013 Helsinki Declaration and was approved by the Hospitals' Review Boards. All participants provided written informed consent for the study.

ORCID

Sara Latrofa http://orcid.org/0009-0004-3514-8774
Paolo Seghetti http://orcid.org/0000-0001-5965-6539
Martina Modena http://orcid.org/0000-0003-0555-542X

REFERENCES

1. Brugada P, Brugada J. Right bundle branch block, persistent ST segment elevation and sudden cardiac death: a distinct clinical and electrocardiographic syndrome. *J Am Coll Cardiol*. 1992;20:1391-1396.
2. Meregalli P, Wilde A, Tan H. Pathophysiological mechanisms of Brugada syndrome: depolarization disorder, repolarization disorder, or more? *Cardiovasc Res*. 2005;67:367-378.
3. Tukkie R, Sogaard P, Vleugels J, de Groot IKLM, Wilde AAM, Tan HL. Delay in right ventricular activation contributes to Brugada syndrome. *Circulation*. 2004;109:1272-1277.
4. Emori T, Antzelevitch C. Cellular basis for complex T waves and arrhythmic activity following combined IKr and IKs block. *J Cardiovasc Electrophysiol*. 2001;12:1369-1378.
5. Tse G, Gong M, Li CKH, et al. Tpeak-Tend, Tpeak-Tend/QT ratio and Tpeak-Tend dispersion for risk stratification in Brugada syndrome: a systematic review and meta-analysis. *J Arrhythm*. 2018;34:587-597.
6. Wyatt RF, Burgess MJ, Evans AK, Lux RL, Abildskov JA, Tsutsumi T. Estimation of ventricular transmembrane action potential durations and repolarization times from unipolar electrograms. *Am J Cardiol*. 1981;47:488.
7. Pannone L, Monaco C, Ramak R, et al. New insights into risk stratification of Brugada syndrome from high density epicardial electroanatomic mapping. *Eur Heart J*. 2021;42:638.
8. Zhang P, Tung R, Zhang Z, et al. Characterization of the epicardial substrate for catheter ablation of Brugada syndrome. *Heart Rhythm*. 2016;13:2151-2158.
9. Nagase S, Kusano KF, Morita H, et al. Longer repolarization in the epicardium at the right ventricular outflow tract causes type 1 electrocardiogram in patients with Brugada syndrome. *J Am Coll Cardiol*. 2008;51:1154-1161.
10. Lambiase PD, Ahmed AK, Ciaccio EJ, et al. High-density substrate mapping in Brugada syndrome: combined role of conduction and repolarization heterogeneities in arrhythmogenesis. *Circulation*. 2009;120:106-117.
11. Leong KMW, Ng FS, Yao C, et al. ST-elevation magnitude correlates with right ventricular outflow tract conduction delay in Type I Brugada ECG. *Circ Arrhythm Electrophysiol*. 2017;10:e005107.
12. Priori SG, Wilde AA, Horie M, et al. HRS/EHRA/APHRS expert consensus statement on the diagnosis and management of patients with inherited primary arrhythmia syndromes. *Heart Rhythm*. 2013;10:1932-1963.
13. Zeppenfeld K, Tfelt-Hansen J, de Riva M, et al. 2022 ESC guidelines for the management of patients with ventricular arrhythmias and the prevention of sudden cardiac death. *Eur Heart J*. 2022;43:3997-4126.
14. Sroubek J, Probst V, Mazzanti A, et al. Programmed ventricular stimulation for risk stratification in the Brugada syndrome. *Circulation*. 2016;133:622-630.
15. Letsas KP, Efremidis M, Vlachos K, et al. Right ventricular outflow tract low-voltage areas identify the site of origin of idiopathic ventricular arrhythmias: A high-density mapping study. *J Cardiovasc Electrophysiol*. 2019;30:2362-2369.
16. Williams SE, Roney CH, Connolly A, et al. OpenEP: a cross-platform electroanatomic mapping data format and analysis platform for electrophysiology research. *Front Physiol*. 2021;12:160.
17. Ahrens J, Geveci B, Law C. ParaView: an end-user tool for large data visualization. *The Visualization Handbook*, 2005.
18. Antzelevitch C, Di Diego JM. Tpeak-Tend interval as a marker of arrhythmic risk. *Heart Rhythm*. 2019;16:954-955.
19. Yan GX, Antzelevitch C. Cellular basis for the Brugada syndrome and other mechanisms of arrhythmogenesis associated with ST-segment elevation. *Circulation*. 1999;100:1660-1666.
20. Coronel R, de Bakker JMT, Wilms-Schopman FJG, et al. Monophasic action potentials and activation recovery intervals as measures of ventricular action potential duration: experimental evidence to resolve some controversies. *Heart Rhythm*. 2006;3:1043-1050.
21. Martin CA, Guzadhur L, Grace AA, Lei M, Huang CLH. Mapping of reentrant spontaneous polymorphic ventricular tachycardia in a Scn5a+/- mouse model. *Am J Physiol Heart Circ Physiol*. 2011;300:H1853-H1862.
22. Nademanee K, Veerakul G, Chandanamattha P, et al. Prevention of ventricular fibrillation episodes in Brugada syndrome by catheter ablation over the anterior right ventricular outflow tract epicardium. *Circulation*. 2011;123:1270-1279.
23. Szél T, Antzelevitch C. Abnormal repolarization as the basis for late potentials and fractionated electrograms recorded from epicardium in experimental models of Brugada syndrome. *J Am Coll Cardiol*. 2014;63:2037-2045.
24. Antzelevitch C, Patocskai B. Ajmaline-induced slowing of conduction in the right ventricular outflow tract cannot account for ST elevation in patients with type I Brugada ECG. *Circ Arrhythm Electrophysiol*. 2017;10:e005775.
25. Maury P, Sacher F, Gourraud JB, et al. Increased Tpeak-Tend interval is highly and independently related to arrhythmic events in Brugada syndrome. *Heart Rhythm*. 2015;12:2469-2476.
26. Priori SG, Gasparini M, Napolitano C, et al. Risk stratification in Brugada syndrome. *J Am Coll Cardiol*. 2012;59:37-45.

SUPPORTING INFORMATION

Additional supporting information can be found online in the Supporting Information section at the end of this article.

How to cite this article: Latrofa S, Hartwig V, Bachi L, et al. Endocardial repolarization dispersion in BrS: a novel automatic algorithm for mapping activation recovery interval. *J Cardiovasc Electrophysiol*. 2024;35:965-974. doi:10.1111/jce.16244